

Drop size distribution retrieval from polarimetric radar measurements

E. Gorgucci¹, V. Chandrasekar², and V. N. Bringi²

¹Istituto di Scienze dell'Atmosfera e del Clima, Rome, Italy

²Colorado State University, Fort Collins, Colorado, USA

Abstract. Retrieval of drop size distribution (DSD) parameters is one of the longstanding goals of polarimetric radar measurements. Using a gamma model, estimates for the parameters of the DSD model are developed for S, C, and X band frequencies. The model for mean shape of raindrops is critical to the interpretation of polarimetric radar measurements and DSD retrievals. The shape size relation for raindrops is modeled as an equivalent linear form and the slope of the prevailing shape size relation is also derived. The DSD retrievals are validated using disdrometer data. It is shown that the parameters of the DSD namely drop median diameter (D_0) and the intercept parameter $\log_{10} N_w$ can be estimated to an accuracy of 10%.

1 Introduction

Ever since the introduction of differential reflectivity (Z_{dr}) measurement, one of the long-standing goals of polarimetric radar has been the estimation of the raindrop size distribution (DSD). Seliga and Bringi (1976) showed that Z_{dr} , for an exponential DSD, is directly related to the median volume diameter (D_0). Careful intercomparisons between radar measurements of Z_{dr} and D_0 derived from surface disdrometers and airborne imaging probes have shown that D_0 can be estimated to an accuracy of about 10–15% (see, for example, Aydin et al., 1987; Goddard et al., 1982; Bringi et al., 1998). A general gamma distribution model was suggested by Ulbrich (1983) to characterize the natural variation of the DSD. The specific differential propagation phase (K_{dp}) is a forward scatter measurement whereas Z_{dr} is a backscatter measurement. The weighting of the DSD by Z_{dr} and K_{dp} is controlled by the variation of mean raindrop shape with size. A combination of the three radar measurements (Z_h , Z_{dr} and K_{dp}) can be utilized to estimate the DSD, specifically a parametric form of the DSD such as the gamma DSD.

This paper presents algorithms for the estimation of parameters of a gamma DSD from polarimetric radar measurements at various frequency bands.

2 Raindrop size distribution

The raindrop size distribution describes the probability density/distribution function of raindrop sizes. In practice, the normalized histogram of raindrop sizes (normalized with respect to the total number of observed raindrops) converges to the probability density function of raindrop sizes. A gamma distribution model can adequately describe many of the natural variations in the shape of the raindrop size distribution (Ulbrich, 1983). The gamma raindrop size distribution can be expressed as (Chandrasekar and Bringi, 1987),

$$N(D) = n_c f_D(D) \quad (m^{-3} mm^{-1}) \quad (1)$$

where $N(D)$ is the number of raindrops per unit volume per unit size interval (D to $D + \Delta D$), n_c is the number concentration and $f_D(D)$ is the probability density function (pdf). When $f_d(D)$ is of the gamma form it is given by,

$$f_D(D) = \frac{\Lambda^{\mu+1}}{\Gamma(\mu+1)} e^{-\Lambda D} D^\mu, \quad \mu > -1 \quad (2)$$

where Λ and μ are the parameters of the gamma pdf. Any other gamma form such as the one introduced by Ulbrich (1983),

$$n(D) = N_0 D^\mu e^{-\Lambda D} \quad (3)$$

can be derived from this fundamental notion of raindrop size distribution. It must be noted that any function used to describe $N(D)$ when integrated over D must yield the total number concentration, to qualify as a DSD function. This property is a direct consequence of the fundamental result that any probability density function must integrate to unity. The relation between D_0 , μ and Λ is given by

$$\Lambda D_0 \cong 3.67 + \mu. \quad (4)$$

Similarly, a mass-weighted mean diameter D_m can be defined as

$$D_m = \frac{E(D^4)}{E(D^3)} \quad (5)$$

where E stands for the expected value. Using (4), $f_D(D)$, the gamma pdf described by (2), can be written in terms of D_0 and μ as,

$$f_D(D) = \frac{(3.67 + \mu)^{\mu+1}}{\Gamma(\mu+1)D_0} \cdot \left(\frac{D}{D_0}\right)^\mu e^{-[(3.67+\mu)\frac{D}{D_0}]} \quad (6)$$

The above form makes the normalized diameter (D/D_0) as the variable rather than D . Several measurables such as water content (W) and rainfall rate (R) can be expressed in terms of the DSD.

In order to compare the pdf of D (or, $f_D(D)$) in the presence of varying water contents, the concept of scaling the DSD has been used by several authors (Sekhon and Srivastava, 1971; Willis, 1984; and Testud et al., 2000, Bringi and Chandrasekar, 2001, Illingworth and Blackman, 2002). The corresponding form of $N(D)$ can be expressed as,

$$N(D) = N_w f(\mu) \left(\frac{D}{D_0}\right)^\mu \exp\left[-(3.67 + \mu)\frac{D}{D_0}\right] \quad (7)$$

where N_w is the scaled version of N_0 defined in (3),

$$N_w = \frac{N_0}{f(\mu)} D_0^\mu \quad (8)$$

and

$$f(\mu) = \frac{6}{(3.67)^4} \cdot \frac{(3.67 + \mu)^{\mu+4}}{\Gamma(\mu+4)} \quad (9)$$

with $f(0)$ and $f(\mu)$ is a unit less function of μ . One interpretation of N_w is that it is the intercept of an equivalent exponential distribution with the same water content and D_0 as the gamma DSD. (Bringi and Chandrasekar, 2001). Thus N_w , D_0 and μ form the three parameters of the gamma DSD.

3 Raindrop shape and implication for polarimetric radar measurements

The equilibrium shape of raindrops is determined by a balance of hydrostatic, surface tension and aerodynamic forces. The commonly used model for raindrops assumes oblate spheroidal shapes, with the axis ratio b/a , where b and a are the semi-minor and the semi-major axis lengths, respectively. Pruppacher and Beard (1970) give a simple model for the axis ratio (r) based on a linear fit to wind tunnel data as,

$$r = 1.03 - 0.062D; \quad 1 \leq D \leq 9\text{mm}. \quad (10)$$

Rotating linear polarization data in heavy rain (Hendry et al., 1987) has indicated that raindrops fall with the mean orientation of their symmetry axis in the vertical direction. The large swing in the crosspolar power in their data implies a high degree of orientation of drops with the standard deviation of canting angles estimated to be around 6° assuming a Gaussian model. It is reasonable to assume that the standard deviation of canting angles is in the range 5 – 10° (Bringi and Chandrasekar, 2001).

3.1 Differential reflectivity

The differential reflectivity can be written as (Seliga and Bringi, 1976),

$$Z_{dr} = 10 \log_{10} \frac{E[\sigma_{hh}(D)]}{E[\sigma_{vv}(D)]} = 10 \log_{10}(\xi_{dr}) \quad (11)$$

where the symbol E represents expectation and σ_{hh} and σ_{vv} are the cross sections at horizontal and vertical polarizations, respectively. Seliga and Bringi (1976) showed that for an exponential distribution and axis ratio given by (10), Z_{dr} could be expressed as a function of the median volume diameter D_0 . This microphysical link between a radar measurement and a parameter of the DSD is important. For a more general gamma form an approximate power law fit can be derived assuming $-1 \leq \mu \leq 5$, $0.5 < D_0 < 2.5$ mm and N_w chosen to be consistent with thunderstorm rain rates. Using the Beard and Chuang (1987) equilibrium shapes power law fits to D_0 and D_m can be derived as,

$$D_0 = 1.619(Z_{dr})^{0.485} \quad (\text{mm}) \quad (12)$$

$$D_m = 1.529(Z_{dr})^{0.467} \quad (\text{mm}) \quad (13)$$

where Z_{dr} is in decibels and the fits are valid at S band frequency (near 3 GHz, Bringi and Chandrasekar, 2001).

3.2 Specific differential phase

K_{dp} can be related to the water content as (Bringi and Chandrasekar, 2001)

$$K_{dp} = \left(\frac{180}{\lambda}\right) \cdot 10^{-3} \cdot c \cdot W(1 - \bar{r}_m) \quad (\text{deg} \cdot \text{km}^{-1}) \quad (14)$$

where $c \cong 3.75$ is both dimensionless and independent of wavelength. This result links the specific differential phase with parameters of the DSD. If the slope for of shape size relation corresponding to equilibrium value (.062) is used in (14) of the then K_{dp} is given by,

$$K_{dp} = \left(\frac{180}{\lambda}\right) \cdot 10^{-3} \cdot c \cdot W(0.062)D_m(\text{deg} \cdot \text{km}^{-1}) \quad (15)$$

Thus K_{dp} is related to the product of D_m and water content. Though the above result was obtained using the Rayleigh-Gans approximation, it is valid up to 13 GHz (Bringi and Chandrasekar, 2001).

3.3 Mean raindrop shape derived from polarimetric radar measurements

Gorgucci et al. (2000) assumed a simple linear model for axis ratio versus size of the form,

$$r = 1 - \beta D \quad (16)$$

and derived radar-based estimators of β .

Let $p(r)$ be the probability density function of the axis ratio for a given diameter (about a mean value such as that

Table 1. The coefficients of D_0 estimator (in Eq. (19)) at S, C, and X band

| Coefficients | a_1 | b_1 | c_1 |
|--------------|-------|-------|----------------------|
| S | 0.56 | 0.064 | $0.024\beta^{-1.42}$ |
| C | 0.59 | 0.083 | $0.021\beta^{-1.16}$ |
| X | 0.627 | 0.057 | $0.03\beta^{-1.22}$ |

given by Eq. 16). The expression for K_{dp} can be generalized as (Bringi and Chandrasekar, 2001),

$$K_{dp} = \frac{2\pi c'}{k_0} \int D^3 N(D) \int (1-r)p(r)dr dD \quad (17)$$

$$= \frac{2\pi c'}{k_0} \int D^3 N(D) [1 - E(r)] dD \quad (18)$$

where $E(r)$ is the mean value of r , and c' is a constant. The functional dependence of $E(r)$ versus D may be modeled as in (16). Using the linear model in (16), Gorgucci et al. (2000) showed the variations of Z_{dr} and K_{dp} with respect to β , and in turn derived an estimator for β based on polarimetric radar measurements. This can be used subsequently in algorithms relating Z_{dr} and K_{dp} to the parameters of the DSD, which gives rise to a methodology for estimating the gamma DSD parameters based on radar measurements.

4 Estimators of the gamma DSD parameters

Seliga and Bringi (1976) showed that for an exponential distribution, the two parameters of the DSD, namely N_w and D_0 , can be estimated using Z_{dr} and Z_h . They used a two-step procedure where they estimated D_0 using an equilibrium raindrop shape model and subsequently used that in the expression for Z_h to estimate N_w . This procedure can essentially be applied for a gamma DSD, and generalized to account for raindrop oscillations using the linear model in (16). The procedure for estimating the gamma DSD parameters is as follows: first estimate β using the algorithm described by Gorgucci et al. (2000), and subsequently, estimate D_0 , N_w and μ recognizing the prevailing β value. Using simulations Gorgucci et al. derived an estimator for \hat{D}_0 at S-band as,

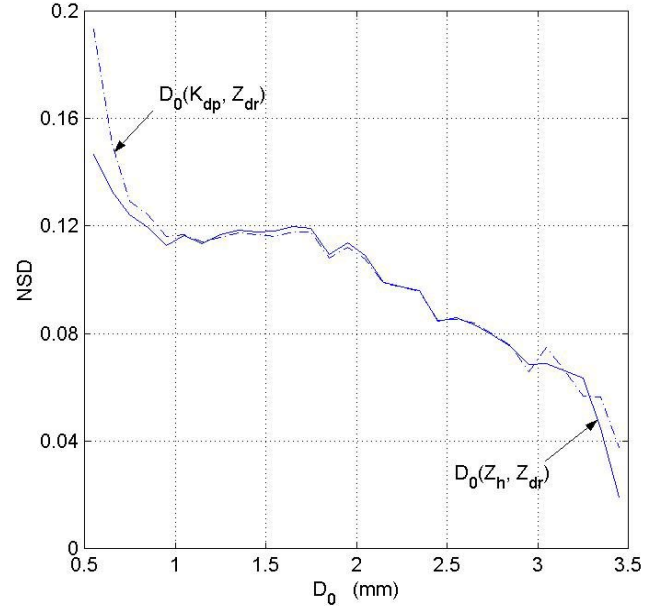
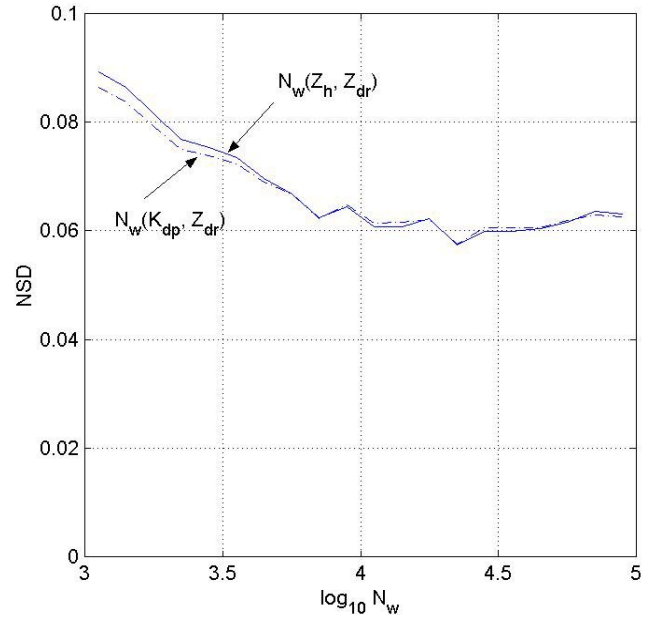
$$\hat{D}_0 = a_1 Z_h^{b_1} (\xi_{dr})^{c_1}. \quad (19)$$

These coefficients for S-band are

$$a_1 = 0.56, \quad b_1 = 0.064, \quad c_1 = 0.024\beta^{-1.42}. \quad (20)$$

Similar estimates can be derived for C and X band using the corresponding expression for C and X band given in Table 1.

Simulations can also be utilized to evaluate the performance of the estimator of D_0 in (19). Quantitative analysis of the simulations gives a correlation coefficient of 0.963. Figure 1 shows the normalized standard deviation (NSD) of \hat{D}_0 as a function of D_0 . It can be seen from Fig. 1 that D_0 can be estimated to an accuracy of about 10% when $D_0 >$

**Fig. 1.** Normalized standard deviation (NSD) in the estimates of D_0 as a function of the true value of D_0 .**Fig. 2.** Normalized standard deviation in the estimates of $\log_{10} N_w$, as a function of $\log_{10} N_w$.

1 mm. The corresponding parameters at C and X band are as follows. The correlation coefficients are 0.93 and 0.95, whereas the normalized standard errors are 15% and 13% respectively.

4.1 Estimation of N_w

Once D_0 is estimated, N_w can be easily estimated using one of the moments of the DSD such as Z_h or K_{dp} . For example,

Table 2. The coefficients of N_w estimator (in Eq. (22)) at S, C, and X band

| Coefficients | a_1 | b_1 | c_1 |
|--------------|-------|-------|------------------------|
| S | 3.29 | 0.058 | $-0.023\beta^{-1.389}$ |
| C | 3.01 | 0.054 | $-0.02\beta^{-1.25}$ |
| X | 2.97 | 0.07 | $-0.0294\beta^{-1.26}$ |

Z_h can be written in terms of the gamma DSD parameters as,

$$\frac{Z_h}{N_w} = F_z(\mu) D_0^7. \quad (21)$$

Thus it can be seen that N_w can be estimated in terms of D_0 . However, the estimate of D_0 can be obtained in terms of Z_h and Z_{dr} (or K_{dp} and Z_{dr}). Therefore, a direct estimate of N_w can be pursued of the form,

$$\log_{10}(N_w) = a_2 Z_h^{b_2} \xi_{dr}^{c_2}. \quad (22)$$

The variability of a_2 , b_2 , c_2 can be parameterized in terms of β at S band as

$$a_2 = 3.29, \quad b_2 = 0.058, \quad c_2 = -0.023\beta^{-1.389}. \quad (23)$$

In summary, the estimator for N_w is obtained as follows. Using Z_h , Z_{dr} and K_{dp} first estimate β . Subsequently, calculate the coefficients in (23) and use in (22) to estimate N_w . Quantitative analysis of the scatter yields a correlation coefficient of 0.831. Figure 2 shows the NSD of N_w as a function of $\log_{10} N_w$. It can be seen, from Fig. 2, that $\log_{10} N_w$ is estimated to a normalized standard deviation of better than 7% when $\log_{10} N_w > 3.5$. Note that due to the wide variability of N_w , $\log_{10} N_w$ is the preferred scale of comparison (similar to dB scale for reflectivity). At C and X bands the parameterization for N_w can be obtained in a similar manner and the results are summarized in Table 2. The normalized standard deviation in the estimate of $\log_{10} N_w$ using K_{dp} and Z_{dr} is also shown in Fig. 2. It can be seen from Fig. 2 that the two estimators for $\log_{10} N_w$ works fairly well.

4.2 Parameterization of μ

The parameter μ describes the overall shape of the distribution. Once D_0 is estimated, μ can be estimated from parameterization, which is skipped here for brevity. Estimating μ accurately under practical conditions, especially in the presence of measurement errors is very difficult using the procedures discussed here.

5 Impact of measurement error on the estimates of D_0 and N_w

Estimators of D_0 use measurements of Z_h , Z_{dr} , and K_{dp} . Any error in the measurement of these three parameters will directly translate into errors in the estimates of D_0 and N_w .

The three measurements Z_h , Z_{dr} , and K_{dp} have completely different error structures.

The Z_h is based on absolute power measurement and has a typical accuracy of 1 dB. The Z_{dr} is a relative power measurement, which can be estimated to an accuracy of about 0.2 dB. K_{dp} is the slope of the range profile of the differential propagation phase Φ_{dp} , which can be estimated to an accuracy of a few degrees. The subsequent estimate of K_{dp} depends on the procedure used to compute the range derivative of Φ_{dp} such as a simple finite-difference scheme or a least squares fit. Using a least squares estimate of the Φ_{dp} profile, the standard deviation of K_{dp} can be expressed as (Gorgucci et al., 1999),

$$\sigma(K_{dp}) = \sqrt{3} \frac{\sigma(\Phi_{dp})}{N \Delta r} \sqrt{\frac{N}{(N-1)(N+1)}}, \quad (24)$$

where Δr is the range resolution of the Φ_{dp} estimate and N is the number of range samples along the path. For a typical 150 m range spacing, and with 2.5° accuracy of Φ_{dp} , K_{dp} can be estimated over a path of 3 km, with a standard error of $0.32^\circ \text{ km}^{-1}$.

The measurement errors of Z_h , Z_{dr} , and K_{dp} are nearly independent. Simulations were used to quantify the error structure of the estimates of D_0 and N_w . The normalized standard deviation in the estimates of D_0 and N_w including the effect of measurement error were evaluated. The analysis shows that in general, there is about a 10% increase in the NSD of D_0 estimate due to measurement error. Similarly there is a 4% to 16% increase in the error of N_w depending on the value of N_w . These errors can be further reduced using other techniques such as spatial averaging whenever possible. The following section presents evaluation of the algorithms developed here using disdrometer observations.

6 Evaluation of the algorithms using disdrometer data, and application to radar data

6.1 Evaluation using disdrometer data

The algorithms developed in this paper to estimate D_0 and N_w are applied to data collected with a J-W impact disdrometer (Joss and Waldvogel, 1967) during a rainfall season (covering about three months) from Darwin (Australia). This data set was collected by the Bureau of Meteorology Research Center (BMRC) and includes a variety of rainfall types from a tropical regime with rain rates between 1 to 150 mm h⁻¹. The disdrometer data consists of measurements of $N(D)$ in discrete intervals of ΔD at 30 seconds intervals which are subsequently averaged over 2 minutes. While several methods are available to fit the measured $N(D)$ to a gamma form (e.g. Willis, 1984), the method used here is based on Bringi and Chandrasekar (2001). Once the set of (N_w, D_0, μ) parameters are obtained, the radar observables Z_h , Z_{dr} and K_{dp} are simulated based on the following assumptions:

1. Axis ratio versus D relation based on the fit proposed by Andsager et al. (1999).
2. Gaussian canting angle distribution with mean of 0° and standard deviation 10° .
3. Truncation of the gamma DSD at $D_{max} = 3.5 D_m$.

The simulated set of radar observables (Z_h , Z_{dr} and K_{dp}) gives an “effective” β of 0.0475 (for comparison the equilibrium β is 0.062).

Note that the algorithms for D_0 and N_w are constructed to be insensitive to the actual value of β , so that the details of the assumptions used in simulating the set of radar observables are not of particular relevance, and this fact is indeed the power of the proposed D_0 and N_w algorithms. In order to evaluate these algorithms using disdrometer measurements, the simulated values of Z_h , Z_{dr} and K_{dp} are used to calculate \hat{D}_0 , \hat{N}_w and $\hat{\mu}$ which are then compared against D_0 , N_w and μ estimated by gamma fits to the set of measured $N(D)$. Disdrometer analysis showed that \hat{D}_0 can be estimated to $NSD < 7\%$ especially for $D_0 > 1$ mm. As expected the D_0 estimates get very accurate for higher values. The $\log_{10}(N_w)$ comparison shows that the accuracy in the retrieval of $\log_{10} N_w$ is quite high ($< 5\%$) for $N_w > 1000 \text{ mm}^{-1} \text{ m}^{-3}$ (for reference the Marshall-Palmer value for N_w is $8000 \text{ mm}^{-1} \text{ m}^{-3}$).

6.2 Application to radar data

The algorithms described in this paper can be directly applied to radar data and an example as applied to TRMM (Tropical Rainfall Measurement Mission) is shown here. Figure 3a shows the ground radar data of reflectivity with coincident TRMM radar beam plotted over it. Figure 3b shows the corresponding plots of DSD estimates along the TRMM radar beam (PR) evaluated for comparison against PR retrievals.

7 Summary and conclusions

One of the long-standing goals of polarimetric radar has been the estimation of the parameters of the raindrop size distribution. Estimators for the parameters of a three-parameter gamma model, namely D_0 , N_w and μ are developed in this paper based on the radar observations Z_h , Z_{dr} and K_{dp} . It should be noted that the DSD estimates computed here correspond to radar measurements from the radar resolution volume. Statistical analysis of the estimator of D_0 indicates that it can be estimated to an accuracy of 10% when D_0 is 2 mm (and similar accuracies at the other D_0 values). Once D_0 is estimated, other measurements such as Z_h or K_{dp} can be used to estimate $\log_{10} N_w$, to a normalized standard deviation of about 6.5% when $N_w = 8000 \text{ mm}^{-1} \text{ m}^{-3}$ and similar order at the other values.

The estimation of μ is not easy because of the least influence of this parameter on the three measurements Z_h , Z_{dr} and K_{dp} . Therefore; the parametric estimates of μ derived

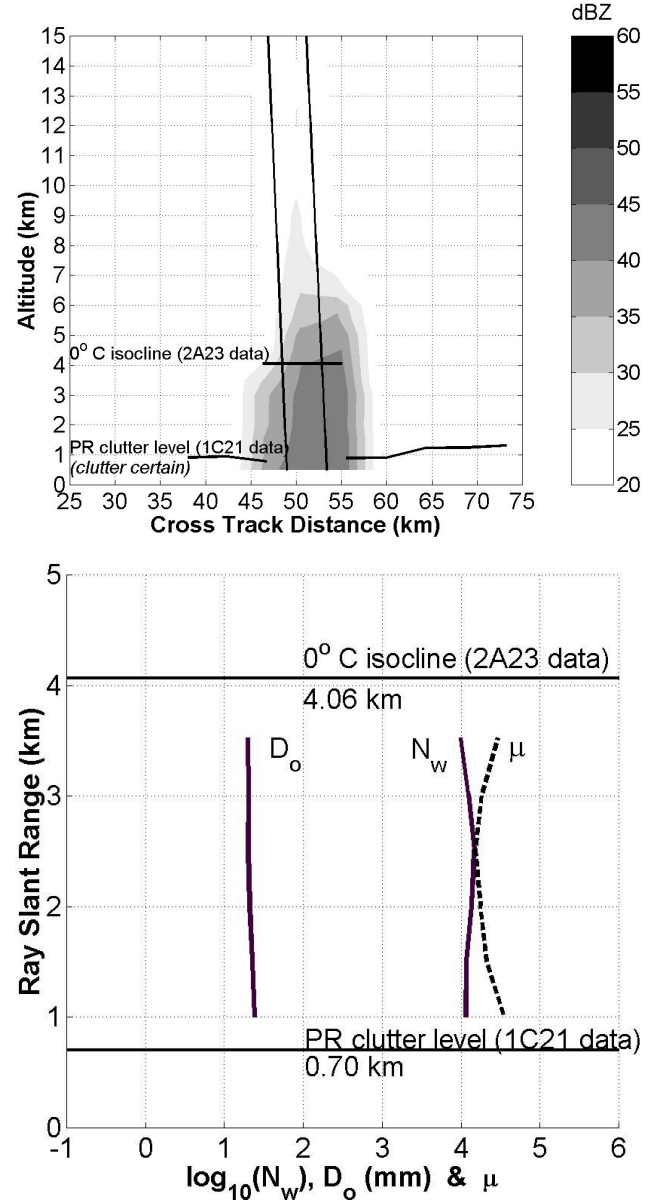


Fig. 3. (a) Example of ground based observations and RSD estimates from using TRMM-LBA storm cell. Vertical profile of GR reflectivity with location of PR beam indicated by solid vertical lines drawn to scale. (b) Estimates of the RSD along PR ray corresponding to the ray indicated in panel (a) for altitudes between the PR clutter level and isocline height. Solid vertical lines indicate D_0 , and N_w (as labeled), while the dotted is the parameter, μ . In all panels, solid horizontal lines indicate the 0° C isocline altitude and the PR clutter level (certain), as derived from the PR2A25 and 1C21 data products, respectively.

are not as accurate. At low rain rates K_{dp} is noisy. Therefore a hybrid approach is implemented in this paper. When $K_{dp} \leq 0.2 \text{ deg. km}^{-1}$, Bringi et al. (2002) have extended this procedure to low rain rates. The algorithms developed here were applied to one rainy season of disdrometer data collected in Darwin, Australia. The disdrometer analysis indicates that the algorithms work fairly well for the estimation

of D_0 and N_w . In summary, the algorithms presented in this paper can be used to estimate the parameters of the raindrop size distribution, from polarimetric radar data at a frequency near 3 GHz (S-band), directly. However at C and X bands attenuation correction needs to be introduced, prior to DSD estimation

Acknowledgement. Two of the authors (VC and VNB) acknowledge support from the NASA TRMM program. This research was supported partially by the National Group for Defense from Hydrological Hazard (CNR, Italy) and by the Italian Space Agency (ASI). The disdrometer data were provided by Dr. T. Keenan of the Bureau of Meteorology Research Center. The authors acknowledge Dr. S. Bolen of NASA for assistance with the analysis of TRMM data.

References

- Andsager, K., K. V. Beard and N. F. Laird: Laboratory measurements of axis ratios for large raindrops. *J. Atmos. Sci.*, 56, 2673–2683, 1999.
- Aydin, K., H. Direskeneli, and T. A. Seliga: Dual-polarization radar estimation of rainfall parameters compared with ground-based disdrometer measurements: 29 October 1982, Central Illinois experiment. *IEEE Trans. Geosci. Remote Sens.*, GE-25, 834–844, 1987.
- Beard, K. V., and C. Chuang: A new model for the equilibrium shape of raindrops. *J. Atmos. Sci.*, 44, 1509–1524, 1987.
- Bringi, V. N., V. Chandrasekar, and R. Xiao: Raindrop axis ratio and size distributions in Florida rainshafts: an assessment of multiparameter radar algorithms. *IEEE Trans. Geosci. Remote Sensing*, 36, 703–715, 1998.
- Bringi, V. N. and V. Chandrasekar: *Polarimetric Doppler Weather Radar: Principles and Applications*. Cambridge University Press, 636 pp, 2001.
- Bringi, V. N., Gwo-Jong Huang, V. Chandrasekar, E. Gorgucci: A Methodology for Estimating the Parameters of a Gamma Raindrop Size Distribution Model from Polarimetric Radar Data: Application to a Squall-Line Event from the TRMM/Brazil Campaign. *J. Atmos. Oceanic Technol.*, 19, 633–645, 2002.
- Chandrasekar, V., and V. N. Bringi: Simulation of Radar Reflectivity and Surface Measurements of Rainfall. *J. Atmos. Oceanic Technol.*, 464–478, 1987.
- Goddard, J. W. F., S. M. Cherry, and V. N. Bringi: Comparison of dual-polarization measurements of rain with ground-based disdrometer measurements. *J. Appl. Meteor.*, 21, 252–256, 1982.
- Gorgucci, E., G. Scarchilli, and V. Chandrasekar: Specific differential phase shift estimation in the presence of non-uniform rainfall medium along the path. *J. Atmos. Oceanic Technol.*, 16, 1690–1697, 1999.
- Gorgucci, E., G. Scarchilli, and V. Chandrasekar: Measurement of mean raindrop shape from polarimetric radar observations. *J. Atmos. Sci.*, 57, 3406–3413, 2000.
- Gunn, R. and G. D. Kinzer: The terminal velocity of fall for water droplets in stagnant air. *J. Meteor.*, 6, 243–248, 1949.
- Hendry, A., Y. M. M. Antar, and G. C. McCormick: On the relationship between the degree of preferred orientation in precipitation and dual polarization radar echo characteristics. *Radio Sci.*, 22, 37–50, 1987.
- Illingworth, Anthony J., T. Mark Blackman: The Need to Represent Raindrop Size Spectra as Normalized Gamma Distributions for the Interpretation of Polarization Radar Observations. *Journal of Applied Meteorology*: Vol. 41, No. 3, pp. 286–297, 2002.
- Joss, J. and A. Waldvogel: A raindrop spectrograph with automatic analysis. *Pure Appl. Geophys.*, 68, 240–246, 1967.
- Pruppacher, H. R. and K. V. Beard: A wind tunnel investigation of the internal circulation and shape of water drops falling at terminal velocity in air. *Quart. J. Roy. Meteor. Soc.*, 96, 247–256, 1970.
- Sekhon R. S., and R. C. Srivastava: Doppler radar observations of drop-size distributions in a thunderstorm. *J. Atmos. Sci.*, 28, 983–994, 1971.
- Seliga, T.A., and V.N. Bringi: Potential use of the radar reflectivity at orthogonal polarizations for measuring precipitation. *J. Appl. Meteor.*, 15, 69–76, 1976.
- Testud J., E. L. Bouar, E. Obligis, and M. Ali-Mehenni: The rain profiling algorithm applied to polarimetric weather radar. *J. Atmos. Oceanic Technol.*, 17, 332–356, 2000.
- Ulbrich, C. W.: Natural variations in the analytical form of raindrop size distributions. *J. Climate Appl. Meteor.*, 22, 1764–1775, 1983.
- Willis, P. T.: Functional fits to some observed drop size distribution and parameterization of rain. *J. Atmos. Sci.*, 41, 1648–1661, 1984.